

Volumetric-Based Analysis of In-Vivo and Ex-Vivo Quantitative MR Diffusion Parameters in Pancreatic Adenocarcinoma: Correlation with Pathologic Findings

Peerboccus M¹, Van Eycke YR^{2,5}, Gyssele E¹, Verset L³, Lucchesi P¹, Absil J¹, Chao SL⁴, Decaestecker C^{2,5}, Van Laethem JL⁶, Metens T^{1,3} and Bali MA^{1,4}

¹Department of Radiology, Hopital Erasme, Universite Libre de Bruxelles, Brussels, Belgium

²Department of DIA Path Center for Microscopy and Molecular Imaging (CMMI), Universite Libre de Bruxelles, Gosselies, Belgium

³Department of Pathology, Hospital Erasme, Universite Libre de Bruxelles, Brussels, Belgium

⁴Department of Radiology, Institut Jules Bordet, Universite Libre de Bruxelles, Brussels, Belgium

⁵Department of Laboratories of Image, Signal processing and Acoustics (LISA), Ecole polytechnique de Bruxelles, Université Libre de Bruxelles, Brussels, Belgium

⁶Department of Gastroenterology, Hospital Erasme, Universite Libre de Bruxelles, Brussels, Belgium

Received: 04 Jun 2019

Accepted: 24 Jun 2019

Published: 29 Jun 2019

*Corresponding to:

Thierry Metens, Department of Radiology, Hôpital Erasme, Université Libre de Bruxelles, Brussels, Belgium, Tel: +322 5553998, E-mail: thierry.metens@erasme.ulb.ac.be

1. Abstract

1.1. Purpose: Imaging biomarkers are needed to assess modifications in pancreatic adenocarcinoma (PA) induced by stroma-targeted therapies. The study investigates correlations between quantitative diffusion parameters obtained in vivo and ex vivo with a tumour volumetric approach and quantitative pathologic findings including fibrosis, vascular and total nuclear densities in PA.

1.2. Methods: 14 patients with resectable were included after informed consent; diffusion weighted imaging (nine b values:0-1000s/mm²) was performed within 4 days before surgery and ex vivo immediately after tumour resection.

Two readers assessed quantitative diffusion parameters (ADC, D, f: apparent and pure diffusion coefficients; perfusion fraction) after tumour volume segmentation based on b=1000 s/mm² images. Statistics included inter-reader agreement with intraclass correlation coefficients (ICC), non-parametric tests to compare in vivo with ex vivo data and ADC, D, f with histopathology findings.

1.3. Results: Readers agreement was excellent (ICC>0.9). Diffusion parameters were significantly lower ex vivo than in vivo (P=.001); ADC and D differed significantly both in vivo and ex vivo (P=.001). Significant positive Spearman correlations were observed between fibrosis and ADC and D in vivo (respectively rs=0.76 and rs=0.73, P=.002 and P=.003) and ex vivo (both rs=0.72 and P=.004). Negative correlations were observed between total nuclear density and ADC and D ex vivo (both rs=-0.66, P=.011) and between total nuclear density and fibrosis (rs=-0.53, P=.049). There was no correlation between vascular density and diffusion parameters.

1.4. Conclusions: A statistically significant positive correlation between ADC and D and degree of fibrosis was found in PA, indicating the presence of a relatively larger extracellular space when fibrosis increases.

2. Key words: Magnetic resonance imaging; Pancreas; Adenocarcinoma; Diffusion; Fibrosis

Take home message: A statistically significant positive correlation between ADC and D and degree of fibrosis was found in pancreatic adenocarcinoma, indicating the presence of a relatively larger extracellular space when fibrosis increases.

3. Introduction

Pancreatic adenocarcinoma (PA) is the fourth cause of cancer-related death in western countries with an overall 5-year survival rate below 8% [1, 2]. PA is characterized by an extensive stroma reaction along with poor vascularization that promote the creation of a hypoxic environment which may act as a mechanical barrier for drug delivery contributing to treatment failure [3].

Surgery is the only curative treatment. Currently, less than 20% of the patients are eligible for potentially curative resection [1] and chemotherapy or chemoradiation therapy are indicated for unresectable locally advanced and metastatic PA [2]. Studies evaluating the association of stroma-targeted drugs with conventional cytotoxic chemotherapy have reported encouraging results, with significant reduction of the stroma, decreased intra-tumoural pressure, increased perfusion and drug delivery [4].

RECIST, the currently used imaging criteria to monitor tumour response to conventional anticancer cytotoxic drugs is based on morphological assessment, i.e. size modification using a one-dimensional measurement of the tumour (longest diameter) [5]. However these criteria may not be appropriate when anti-cancer agents with a novel model of action are administered.

Thus, there is an unmet need of new imaging biomarkers in order to follow up modification of different PA tumour components induced by stroma-targeted therapies. These therapies aim at counteracting tumour growth and invasion promoted by PA stromal cells. Diffusion-Weighted magnetic resonance Imaging (DWI) may reveal as a potential imaging tool in this setting. DWI is sensitive to microscopic movements of water molecules within biological tissue, which reflect tissue cellularity, tortuosity of the extracellular space, integrity of cell membranes and viscosity of fluids. The image contrast on DWI derives from differences in mobility of water molecules within tissues [6]. Several quantitative parameters are derived: the apparent diffusion coefficient, ADC, calculated using a mono-exponential fitting, which is a combined measure of the movement of water molecules within the intra and extracellular spaces (true diffusion) and the intravascular space (flow-related pseudo-perfusion). Alternatively, applying a biexponential model (Intra-Voxel Incoherent Motion, IVIM) allows the separation between the true diffusion and the pseudo-perfusion [7].

Results from previous studies which have assessed the correlation

between PA histopathological characteristics and ADC are conflicting: some described a negative association [8-10], while others did not demonstrate any association [11, 12] or suggested a positive association between ADC and tumoral fibrosis [13].

In view of these contradictory results, further studies are definitely needed. Hence the aim of the present study is to investigate possible correlations between IVIM diffusion parameters obtained in vivo and ex vivo using a volumetric approach and pathologic findings including fibrosis, vascular and total nuclear densities in patients with PA.

4. Material and Methods

This prospective study was approved by the institutional review board and informed consent was obtained from all participants. 14 consecutive patients, 7 men (mean age: 66 years; range: 36–82 years) and 7 women (mean

age: 69 years; range: 55–82 years), were enrolled. The inclusion criteria consisted of the presence of a resectable pancreatic solid tumour with histopathology confirmation of PA. Previous chemotherapy and chemoradiation therapy represented exclusion criteria together with common contraindications to MR examination.

4.1. MR Acquisitions

In vivo MR investigations were carried out on all patients within 4 days before surgery and were performed on a 1.5-Tesla magnet (Achieva; Philips Healthcare, Best, The Netherlands) equipped with a 16-channel phased-array coil. All patients were placed in the magnet in the supine position.

Morphologic images were acquired with transverse and coronal respiratory-triggered T2weighted single-shot turbo spin-echo (SS-TSE), covering the upper abdomen (TE=80ms, echo train length 72, 40 slices, no gap, field-of-view 400x400mm², acquisition voxel 1.8x1x5mm³, Sense-acceleration=2).

Diffusion-weighted MR images were acquired with a transverse respiratory-triggered spin echo echo-planar (SE-EPI) sequence (TE=70ms, echo train length 61, 40 slices, no gap, field-of-view 400x400mm², acquisition voxel 2.3x3x5mm³, Sense-acceleration=2). A spatial-selective inversion recovery prepulse provided fat suppression (TI=180ms). Diffusion-probing gradients with b values of 0, 10, 20, 30, 40, 50, 150, 300 and 1000s/mm² were applied in three orthogonal directions. For each b value the isotropic mean image was reconstructed. The whole MR examination lasted approximately 30 minutes.

The resected pancreatic specimens were scanned within 3 hours ensuing surgery and before histopathology procedures. Ex vivo

MR investigations were carried out with the same magnet as above using a 2-channel phased-array coil.

Morphologic images were acquired with SS-TSE sequences, covering the whole surgical specimen in transverse (20 slices, field-of-view $120 \times 89 \text{ mm}^2$) and coronal (12 slices, field-of-view $120 \times 111 \text{ mm}^2$) orientations (TE=100ms, echo train length 14, no gap, acquisition voxel $0.6 \times 0.9 \times 4.0 \text{ mm}^3$, Sense-acceleration=2).

Diffusion-weighted MR images were acquired with a transverse SE-EPI sequence (TE=70ms, echo train length 17, 15 slices, no gap, field-of-view $100 \times 53 \text{ mm}^2$, acquisition voxel $1.5 \times 1.9 \times 4.0 \text{ mm}^3$, Sense-acceleration=2, TI=180ms, same b values as in vivo).

Image analysis was performed independently by two readers (both were 5th-year radiology

residents - MP, EG) with 1 year of experience in abdominal MR imaging.

An image J-based software [14] was used with a specific graphical user interface [15] to segment the whole tumour volume and calculate diffusion parameters. DW-images acquired with $b=1000 \text{ s/mm}^2$ were used for segmentation. User-defined boxes were manually fitted around the whole tumour which was automatically segmented by thresholding all the inner voxels holding a signal value over the mean +0.5 standard deviation. The resulted volume was manually readjusted on the basis of $b=0 \text{ s/mm}^2$ DW images and T2-weighted images so that the whole tumour was enclosed while avoiding contiguous lymph nodes, non-tumoural tissue, biliary or pancreatic ducts and distortion artefacts on ex vivo images (**Figure 1**).



Figure 1a. In vivo axial T2-weighted image showing a solid tumour in the pancreatic tail.

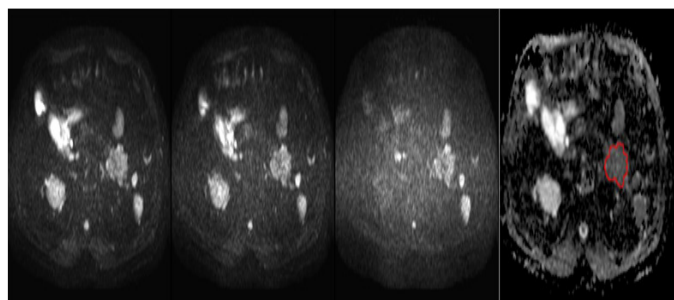


Figure 1b. Corresponding DW images ($b=150, 300$ and 1000 s/mm^2) and ADC map with tumour segmentation (red contour: intersection between DW-volume and image section).

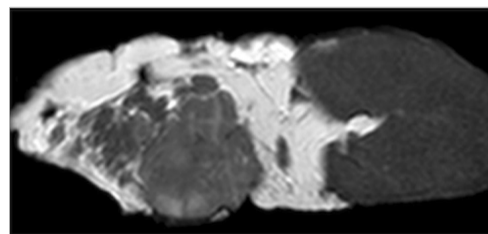


Figure 1c. Ex vivo axial T2-weighted image of the corresponding resected tumour.

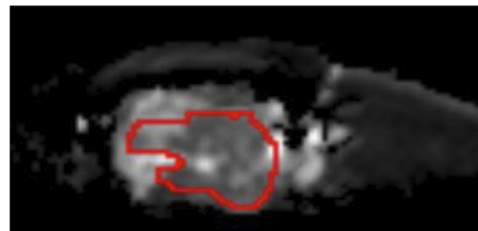


Figure 1d: Corresponding ex vivo ADC map with tumour segmentation (red contour: intersection between DW-volume and image section).

The software calculated the whole tumour volume (DW-volume), from which diffusion parameters were generated.

A mono-exponential model $S(b) = S_0 \exp(-b \text{ ADC})$ including all b values was used to calculate the ADC, whilst a biexponential model $S(b)/S_0 = (1-f) \exp(-bD) + f \exp(-bD^*)$ was employed to derive the pure diffusion coefficient D, the perfusion fraction f and the pseudo-diffusion D^* (D^* was not used in further analysis); $S(b)$ being the signal at a given b value and S_0 being the signal at $b=0 \text{ s/mm}^2$.

The biexponential fit was performed using approximate values of D and f as initial fit value: the initial D value was obtained from a mono-exponential fit involving data from high b values ($b=150$ to 1000 s/mm^2), $S(b) = S_{int} \exp(-bD)$ where S_{int} is the $b=0 \text{ s/mm}^2$ intercept resulting from the fit, while the initial f value was calculated from $f = (S_0 - S_{int}) / S_0$.

The mean values of ADC, D and f were considered for each patient. The analysis was applied to both in vivo and ex vivo images.

4.2. Histopathology Analysis

Histopathology analysis was performed on all 14 surgical specimens by a pathologist with 6 years of experience who was blinded to MR-analysis results.

Surgical specimens were fixed in formalin and cut into contiguous transverse 5-mm thick slices in the cranio-caudal direction carefully aligned to allow a proper comparison with the corresponding transverse DW-images. Tissue blocks containing the tumour were selected (an average of 9 blocks per patient was analyzed) and were cut into serial transverse, 5- μm thick slices for staining to evaluate fibrosis, vascular and nuclear densities. Stained slices from each tumour (9 slices, 1 slice per tumour block) were digitalized at a

magnification of 20x using a calibrated scanner (NanoZoomer, Hamamatsu, Japan). Using image annotations, the pathologist defined different Regions Of Interest (ROI), i.e. the central tumour region (TC) and the peripheral tumour region (TP) as the invading edge of the tumour. The whole tumour region (TW) was defined as the union of TC and TP. Quantification of fibrosis, vascular and nuclear densities was achieved at a magnification of 20x using Visiomorph software (Visiopharm, Denmark). Regions with artefacts, excessive staining or tissue damage were excluded for assessment. Goldner's trichrome staining was performed on a Tissue-Tek DRS 2000 slide stainer (Sakura Finetek Europe B.V., The Netherlands) to detect fibrosis area on each slice (**Figure 2**). Fibrosis density was defined as the ratio of the fibrosis-stained area to the whole tissue area in the ROI. ERG immunohistochemical staining was used to identify endothelial cell nuclei, whereas the other (negative) cell nuclei were evidenced by means of hematoxylin counterstaining (**Figure 3**). Briefly, the slides were subjected to standard IHC (Ventana discovery XT, Roche Diagnostics, Belgium) using the rabbit monoclonal anti-ERG antibody (ready-to-use antibody, clone EPR3864 from Ventana) and the biotin free DAB detection system. Vascular density was defined as the ratio of the ERG-positive nucleus area to that of all (positive or negative) nuclei.

The total nuclear density was defined as the ratio of the total (ERG-positive or negative) nucleus area to the whole tissue area in the ROI. With these definitions the quantification of either fibrosis, vascular or nuclear densities was represented by a single value in TC and in TP.

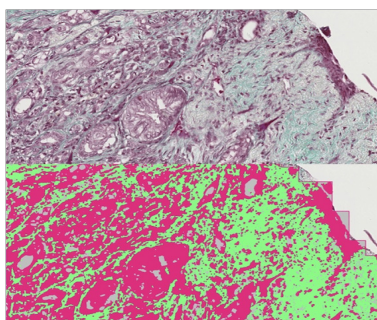


Figure 2: Histopathologic slice of the tumour shown in Figure 1. Assessment of fibrosis density: the upper image is the original image (Goldner's trichrome staining, x20) and the lower one is the processed image, with visualisation of fibrosis in green and the remaining tissue area in dark pink.

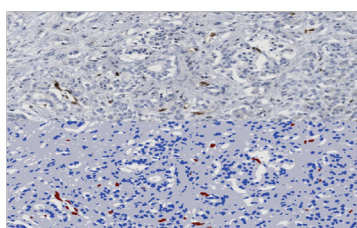


Figure 3: Histopathologic slice of the tumour shown in Figure 1. Assessment of vascular density: the upper image is the original image (ERG immunohistochemical staining with hematoxylin counterstaining, x20), the lower one is the processed image, with negative nuclei coloured in blue and endothelial (positive) nuclei coloured in dark brown. The rest of the tissue is shown in grey.

4.3 Statistical Analysis

Quantitative diffusion parameters, including DW-volume, ADC, D and f calculated in vivo and ex vivo, and histopathology parameters, including fibrosis, vascular and total nuclear densities, were reported as mean and standard deviation.

Intraclass correlation coefficients (ICC) were calculated to assess inter-reader agreement for diffusion parameters.

The non-parametric Wilcoxon's signed rank test was performed to compare paired data samples:

1. *In vivo* and ex vivo values of ADC, D and f
2. ADC and D values
3. Histopathology findings (fibrosis, vascular and total nuclear densities) between TC and TP regions.

The Spearman's rank correlation test was used to assess correlations between:

1. *In vivo* and ex vivo diffusion parameters (ADC, D, f) and histopathology findings (fibrosis, vascular and total nuclear densities)
2. Histopathology findings among them.

The statistical analysis was performed using SPSS (version 23, SPSS, Chicago, Ill) and MedCalc (version 13.1.2, MedCalc Software, Ostend, Belgium).

A P value of 0.05 or less was considered significant.

4.4. Results

Among the 14 respected pancreatic tumours, the histopathology analysis disclosed 12 cases of pancreatic ductal adenocarcinoma, 1 case of pancreatic acinar cell carcinoma and 1 case of pancreatic ductal adenocarcinoma arising from an intra-ductal papillary mucinous neoplasm. Pancreatic tumours were found in the pancreatic head in 12/14 (86%) patients and in the body-tail of the pancreas in 2/14 (14%) patients.

4.4.1. DW-Image Analysis

An excellent agreement was obtained between readers (in vivo ICC=0.95 for ADC, 0.94 for D, 0.99 for f and 0.89 for DW-volume; ex vivo ICC=0.91 for both ADC and D, 0.96 for f and 0.61 for DW-volume). Therefore, measurements from Reader 1 were used for further analysis.

(Table 1) reports mean and standard deviations for DW-volume, ADC, D and f in vivo and ex vivo.

DW-volumes calculated in vivo and ex vivo were not statistically significantly different ($P=.074$). On average, ex vivo volumes were

14% lower than in vivo. Diffusion parameters were significantly lower ex vivo compared with in vivo (all P=.001). A statistically significant difference between ADC and D was also observed both in vivo and ex vivo (both P=.001); the mean difference between ADC and D was 178µm²/s in vivo and 33µm²/s ex vivo (respectively 14% and 4% relative to ADC values).

Table 1: DW-volumes and diffusion parameters calculated in vivo and ex vivo.

(N=14)	In vivo	Ex vivo	P value
DW-volume (cm ³)	15.7 ± 7	13 ± 7.7	0.074
ADC [µm ² /s]	1262 ± 322	771 ± 166	.001*
D [µm ² /s]	1084 ± 263	738 ± 162	.001*
f [%]	24 ± 8	4.25 ± 1.4	.001*

Mean ± standard deviation values are reported with P-values for comparison between in vivo and ex vivo. Wilcoxon's signed rank test, * statistically significant, P≤.05.

4.4.2. Histopathology Analysis

(Table 2) reports histopathology results obtained for fibrosis, vascular and total nuclear densities calculated in TC, TP and TW. A statistically significant difference between TC and TP was observed only for vascular density (P=.030), with higher values in TP. There were no significant differences of fibrosis and total nuclear density between TC and TP.

(Table 3) reports correlations among the histopathology findings. A negative statistically significant correlation was observed between TW fibrosis and TC total nuclear density (P=0.049). A similar trend was observed between TW fibrosis and TW total nuclear density although the correlation did not reach statistical significance (P=.051).

4.4.3. Correlation between quantitative diffusion parameters and histopathology findings

(Table 4) reports correlations between quantitative diffusion parameters calculated in vivo and ex vivo and fibrosis, vascular density and total nuclear density assessed in TC, TP and TW.

Table 2: Histopathology results.

(N=14)	TC	TP	TW
Fibrosis (%)	52 ± 12	52 ± 13	52 ± 11
Vascular density (%)	0.70 ± 0.34	0.98 ± 0.53	0.82 ± 0.41
Total nuclear density (%)	13.5 ± 6	13.9 ± 5	13.5 ± 5

Mean ± standard deviation are given for the central tumour region (TC), the peripheral tumour region (TP) and the whole tumour (TW). The vascular density was significantly higher in TP compared with TC (P=.030).

Table 3: Correlations between fibrosis, vascular density, and total nuclear density calculated in TC, TP and TW.

		TC total nuclear density (%)	TC vascular density (%)	TP total nuclear density (%)	TP vascular density (%)	TW total nuclear density (%)	TW vascular density (%)
TC fibrosis (%)	Correlation Coefficient	-0.411	-0.057	-0.213	0.415	-0.38	0.103
	P value	0.144	0.899	0.464	0.14	0.18	0.725
TP fibrosis (%)	Correlation Coefficient	-0.415	-0.226	-0.464	-0.011	-0.429	-0.178
	P value	0.14	0.436	0.095	0.97	0.126	0.543
TW fibrosis (%)	Correlation Coefficient	-0.534	-0.011	-0.446	0.244	-0.53	0.055
	P value	.049*	0.97	0.11	0.401	0.051	0.852

Spearman's rank correlation test; * statistically significant, P≤.05 TC: central tumour region, TP: peripheral tumour region, TW: whole tumour.

Table 4: Correlations between quantitative diffusion parameters and fibrosis, vascular density, total nuclear density calculated in TC, TP and TW.

		in vivo ADC	in vivo D	in vivo f	ex vivo ADC	ex vivo D	ex vivo f
TC fibrosis (%)	Correlation Coefficient	0.64	0.596	0.253	0.626	0.626	-0.099
	P value	.014*	.025*	0.383	.017*	.017*	0.737
TP fibrosis (%)	Correlation Coefficient	0.705	0.635	0.266	0.604	0.604	-0.301
	P value	.005*	.015*	0.358	.022*	.022*	0.296
TW fibrosis (%)	Correlation Coefficient	0.758	0.732	0.407	0.719	0.719	-0.138
	P value	.002*	.003*	0.149	.004*	.004*	0.637
TC vascular density (%)	Correlation Coefficient	0.007	0.13	-0.138	0.002	0.002	0.073
	P value	0.982	0.659	0.637	0.994	0.994	0.805
TP vascular density (%)	Correlation Coefficient	0.279	0.257	0.024	0.204	0.204	0.002
	P value	0.334	0.375	0.935	0.483	0.483	0.994
TW vascular density (%)	Correlation Coefficient	0.125	0.218	-0.218	0.143	0.143	0.068
	P value	0.67	0.455	0.455	0.626	0.626	0.817
TC total nuclear density (%)	Correlation Coefficient	-0.437	-0.411	-0.231	-0.666	-0.666	-0.055
	P value	0.118	0.144	0.427	.009*	.009*	0.852
TP total nuclear density (%)	Correlation Coefficient	-0.415	-0.415	-0.134	-0.596	-0.596	-0.086
	P value	0.14	0.14	0.648	.025*	.025*	0.771
TW total nuclear density (%)	Correlation Coefficient	-0.486	-0.464	-0.244	-0.657	-0.657	-0.046
	P value	0.078	0.095	0.401	.011*	.011*	0.876

Spearman's rank correlation test; * statistically significant, P≤.05

TC: center of the tumour, TP: peripheral tumour region, TW: whole tumour.

Statistically significant positive correlations were observed between fibrosis and ADC or D both measured in vivo and ex vivo (for P values see table). In contrast, no significant correlation was observed between perfusion fraction f and fibrosis.

No statistically significant correlation was found between vascular density and quantitative diffusion parameters calculated in vivo and ex vivo.

Statistically significant negative correlations were observed between ex vivo ADC or D and total nuclear density. In vivo, negative correlations, although not statistically significant, were also observed between ADC or D and total nuclear density. No

correlation was observed between perfusion fraction f and total nuclear density.

5. Discussion

The main result of our study consisted of statistically significant, moderate to high positive correlations between ADC or D and fibrosis density within PA. This finding was obtained for diffusion measurements performed both *in vivo* and *ex vivo*, using a DW-image based volumetric approach with a careful alignment between histopathologic sections and MR slices.

These results agree with the findings reported by Klauss et al [13] who observed a significant increase in D from moderate to severe degrees of fibrosis in PA.

They suggested that the presence of a more abundant tumoral desmoplastic stroma which embeds the cancer and non-cancer cells constitutes a non-tight, low diffusion restriction microenvironment [13]. So on a comparative basis, a high content of fibrosis will result in less diffusion restriction and in high ADC and D values. Both ADC and D reflect diffusion water motion within the intracellular and extracellular spaces, with the former resulting in a more diffusion restricted environment because of the various structural obstacles within the cell. According to these considerations, we can hypothesize that, as fibrosis increases, both ADC and D may reflect an increase of the extracellular over the intracellular compartment ratio related to the high fibrosis density which is a major histologic feature of PA. Consistently, in our study, a statistically significant, moderate negative correlation was found between TW fibrosis and TC total nuclear density.

These findings suggest the use of these quantitative imaging biomarkers to assess treatment response in PA. Actually, treatment-induced tumoral changes secondary to conventional cytotoxic chemotherapy regimen as well as targeted-therapies such as anti-stroma drugs could be monitored by ADC and D .

However, our findings appear to be in disagreement with other previously published results which reported either a negative correlation between ADC and fibrosis [8-10] or no evidence of correlation [11,12]. Besides the differences in acquisition parameters and post-processing methods between our study and those cited, which could partially explain the difference in results, we agree that ADC is influenced by many factors due to the complex composition of PA microenvironment including cellular density. Importantly, in [8] the degrees of fibrosis were compared only inside a subgroup of moderately differentiated tumors with relatively elevated ADC values. Therefore, correlations between ADC and fibrosis might remain equivocal in absence of the knowledge of these other parameters influencing ADC.

Our study also shows a statistically significant negative, moderate correlation between *ex vivo* ADC or D and total nuclear density.

This relationship has been previously described in both oncologic and non oncologic conditions [16].

The decrease of the *ex vivo* interstitial space (extracellular compartment) due to the loss of fluids and the consequent relative increase of the total nuclear density and thereby total cell density, seems compatible with the higher diffusion restriction and the decrease of respectively ADC and D , confirming previous findings [16].

In vivo, a negative correlation was observed between those same parameters, though not statistically significant: *in vivo* the extracellular compartment of the tissue might contain more water, as confirmed by the higher D value *in vivo* compared to *ex vivo*, its relative volume occupancy might then be more elevated *in vivo* and when the cell density increases, the corresponding decrease in ADC and D might be relatively less important.

While we would expect a correlation between ADC and vascular density and between f and vascular density, both ADC and f being positively influenced by perfusion, no such correlation was found. A possible explanation could be the presence of altered and poorly functional vessels associated with tumor neoangiogenesis, implying that an increase in vascular density does not necessarily yield an increase in perfusion [17].

Statistically significant differences in PA between the DW-derived quantitative parameters calculated respectively *in vivo* and *ex vivo* were observed, with the exception for the DW-volume that as expected did not show any substantial change.

Our study evidenced a statistically significant decrease in ADC, D and f values from *in vivo* to *ex vivo*. Change in tissue microstructure, such as cell swelling due to osmotically driven water flow into cells following ionic imbalance caused by disabled ion pumps may explain the fall of ADC and D values from *in vivo* to *ex vivo* [18]. This leads to a decrease in the extracellular space, while the absence of perfusion in *ex vivo* explains the decrease in perfusion fraction f .

Differences between ADC and D are statistically significant both *in vivo* and *ex vivo*, but more pronounced *in vivo* and the decrease in ADC from *in vivo* to *ex vivo* is more drastic than that in D . There is a two-fold explanation: *in vivo* there is a contribution of the intravascular pseudo-diffusivity to ADC and not to D , and this perfusion-related phenomenon is absent *ex vivo*. Moreover, the statistically significant difference between ADC and D which recurs *ex vivo* may also be due to the fact that D was derived from a biexponential model that is more sensitive to fit error and is probably not appropriated *ex vivo*.

To be as much as possible representative of the whole tumor, from each surgical specimen up to nine blocks containing tumoral tissue have been analyzed at histopathology. All tumors

were subdivided into peripheral and central zones. A statistically significant regional difference was seen only for vascular density that was more pronounced in the peripheral region. As a matter of fact, PA are classically known to be hypovascular tumors and neovascularisation will tend to occur where the tumor is in contact with surrounding non-tumoral tissue, which is more richly supplied with blood [19]. Another explanation could be a high interstitial fluid pressure present within PA due to abnormal angiogenesis, which pushes interstitial fluid from center towards periphery, carrying along proangiogenic factors to the tumor surface where they promote neoangiogenesis [20].

Furthermore, no statistical difference was seen between tumor regions for fibrosis and total nuclear density. To the best of our knowledge, this finding has not been described before. This interesting point, together with the absence of correlation between ADC or D and vascular density, suggests that ADC and D calculated on the whole segmented tumor appear to be representative imaging biomarkers for tumor fibrotic content and cellular density.

Our study has several limitations. The patient cohort is relatively small and this may explain the lack of statistically significant correlations between certain quantitative diffusion parameters and the histopathology features. However, pancreatic cancer is a relatively rare tumor (3.2%/year) with less than 20% of patients candidate for surgery. Moreover, the new oncologic approach to treat borderline patients with neoadjuvant chemotherapy or chemo/radiotherapy has further contributed to the difficulty to recruit treatment-naïve subjects. Also, we did not take into account tumor grade, which according to previous reports seems to have an impact on quantitative diffusion parameters in PA [8,11,12].

In addition, the smaller tumor volume obtained *ex vivo* could be also related to distortion artefacts on diffusion images probably leading to less accurate measurements.

Another limitation is the segmentation method used in our study. It is based on tumor-to-tissue contrast on $b=1000\text{s/mm}^2$ images, aiming at the segmentation of the tumor volume where the diffusivity is lower in the tumor than in the surrounding tissue, which is the case in poorly differentiated PA. This approach may not be accurate when the diffusivity of the tumor is not markedly lower than in the surrounding tissue, as it might be the case in some well differentiated PA. In our study, both $b=0\text{s/mm}^2$ DW-images and T2-weighted images were used to manually readjust the volume segmentation.

Finally, the absence of cardiac triggering during *in vivo* MR acquisition may have an impact on the repeatability and accuracy of perfusion-related measurements.

In conclusion, a statistically significant positive correlation between ADC or D and degree of fibrosis was found in PA, indicating the presence of a relatively larger extracellular space when fibrosis increases. Further studies involving a larger number of patients and investigating the behavior of ADC and D in treatment follow-up are required.

6. Acknowledgments

The CMMI is supported by the European Regional Development Fund and the Walloon Region (« FEDER Wallonie-2020.EU » program, « Wallonia Biomed » portfolio).

C. Decaestecker is a senior research associate with the National (Belgian) Fund for Scientific Research (F.R.S.-FNRS).

The authors would like to thank Dr E Coppens for many discussion related to the study.

References

1. Ryan DP, Hong TS, Bardeesy N. Pancreatic adenocarcinoma. *N Engl J Med.* 2014; 371(11):1039-49.
2. Hidalgo M. Pancreatic cancer. *N Engl J Med.* 2010; 362(17): 1605-17.
3. Neesse A, Michl P, Frese KK et al. Stromal biology and therapy in pancreatic cancer. *Gut.* 2011; 60(6): 861-8.
4. Teague A, Lim KH, Wang-Gillam A. Advanced pancreatic adenocarcinoma: a review of current treatment strategies and developing therapies. *Ther Adv Med Oncol.* 2015; 7(2): 68-84.
5. van Persijn van Meerten EL, Gelderblom H, Bloem JL. RECIST revised: implications for the radiologist. A review article on the modified RECIST guideline. *Eur Radiol.* 2010; 20(6): 1456-67.
6. Koh DM, Collins DJ, Orton MR. Intravoxel incoherent motion in body diffusion-weighted MRI: reality and challenges. *AJR Am J Roentgenol.* 2011; 196(6): 1351-61.
7. Le Bihan D, Breton E, Lallemand D, Aubin ML, Vignaud J, Laval-Jeantet M. Separation of diffusion and perfusion in intravoxel incoherent motion MR imaging. *Radiology.* 1998; 168(2): 497-505.
8. Wang Y, Chen ZE, Nikolaidis P et al. Diffusion-weighted magnetic resonance imaging of pancreatic adenocarcinomas: association with histopathology and tumor grade. *J Magn Reson Imaging.* 2011; 33(1): 136-42.
9. Muraoka N, Uematsu H, Kimura H et al. Apparent diffusion coefficient in pancreatic cancer: characterization and histopathological correlations. *J Magn Reson Imaging.* 2008; 27(6): 1302-8.
10. Hecht EM, Liu MZ, Prince MR, Jambawalikar S, Remotti HE, Weisberg SW et al. Can diffusion-weighted imaging serve as a biomarker of fibrosis in pancreatic adenocarcinoma? *J Magn Reson Imaging.* 2017; 46(2): 393-402.

11. Xie P, Liu K, Peng W, Zhou Z. The Correlation Between Diffusion-Weighted Imaging at 3.0-T Magnetic Resonance Imaging and Histopathology for Pancreatic Ductal Adenocarcinoma. *J Comput Assist Tomogr.* 2015; 39(5): 697-701.
12. Legrand L, Duchatelle V, Molinie V, Boulay-Coletta I, Sibileau E, Zins M. Pancreatic adenocarcinoma: MRI conspicuity and pathologic correlations. *Abdom Imaging.* 2015; 40: 85-94.
13. Klauss M, Gaida MM, Lemke A, et al. Fibrosis and pancreatic lesions: counterintuitive behavior of the diffusion imaging-derived structural diffusion coefficient d . *Invest Radiol.* 2013; 48(3): 129-33.
14. <http://rsb.info.nih.gov/ij/>
15. Chao SL, Metens T, Lemort M. TumourMetrics: a comprehensive clinical solution for the standardization of DCE-MRI analysis in research and routine use. *Quant Imaging Med Surg.* 2017; 7(5): 496-510.
16. Gauvain KM, McKinstry RC, Mukherjee P et al. Evaluating pediatric brain tumor cellularity with diffusion-tensor imaging. *AJR Am J Roentgenol.* 2001; 177(2): 449-54.
17. Fox SB, Harris AL. Histological quantitation of tumour angiogenesis. *APMIS.* 2004; 112(7-8): 413-30.
18. de Crespigny AJ, Rother J, Beaulieu C, Moseley ME, Hoehn M. Rapid monitoring of diffusion, DC potential, and blood oxygenation changes during global ischemia. Effects of hypoglycemia, hyperglycemia, and TTX. *Stroke.* 1999; 30(10):2212-22.
19. Takagi K, Takada T, Amano H. A high peripheral microvessel density count correlates with a poor prognosis in pancreatic cancer. *J Gastroenterol.* 2005; 40(4): 402-8.
20. Rofstad EK, Galappathi K, Mathiesen BS. Tumor interstitial fluid pressure—a link between tumor hypoxia, microvascular density, and lymph node metastasis. *Neoplasia.* 2014; 16(7): 586-94.